

# Temperature Effects on Edge Magnetoplasmons in the Quantum Hall Regime

O. G. Balev<sup>a,b</sup> and Nelson Studart<sup>a</sup>

<sup>a</sup>*Departamento de Física, Universidade Federal de São Carlos,  
13565-905, São Carlos, São Paulo, Brazil*

<sup>b</sup>*Institute of Semiconductor Physics, National Academy of Sciences,  
45 Pr. Nauky, Kiev 252650, Ukraine*

(August 12, 1999)

A *microscopic* treatment of edge magnetoplasmons (EMPs) is presented for the case of not-too-low temperatures in which the inequality  $k_B T \gg \hbar v_g / \ell_0$ , where  $v_g$  is the group velocity of the edge states and  $\ell_0$  is the magnetic length, is fulfilled, and for filling factors  $\nu = 1(2)$ . We have obtained independent EMP modes spatially symmetric and antisymmetric with respect to the edge. We describe in detail the spatial structure and dispersion relations of the new edge waves (edge helicons, dipole, quadrupole and octupole EMPs), which have the characteristic length  $\ell_T = \ell_0^2 k_B T / \hbar v_g$ . We have found that, in contrast to well-known results for a spatially homogeneous dissipation within the channel, the damping of the fundamental EMP at not-too-low temperatures is not quantized and has a  $T^{-1}$  dependence.

PACS 73.20.Dx, 73.40.Hm

## I. INTRODUCTION.

Edge magnetoplasmons (EMPs) in the two-dimensional electron system (2DES) have received much attention in recent years. Experimental studies have been performed to determine the dispersion relation and the role of edge states in the transport properties of the 2DES both on liquid helium [1–3] as in high-mobility AlGaAs-GaAs heterostructures [4–11]. The interest have even increased with the advent of time-resolved transport experiments [7,9,10]. From a theoretical point of view, a lot of work have been also devoted to study the characteristics of these collective excitations propagating along the edge of the 2DES in the presence of a normal magnetic field  $B$  and different edge-wave mechanisms have been proposed [12–23]. First, the EMPs dispersion were determined theoretically within essentially classical models [13,16] in which the charge density varies at the edge, but the edge position of the 2DES is kept constant. Other, distinctly different, quantum-mechanical edge-wave mechanisms was proposed [14,15,17,18] in which only the edge change and the density profile is taken as the unperturbed 2DES with respect to the fluctuating edge.

Recently a microscopic model was proposed in Refs. [21,22] that effectively incorporates the edge-wave mechanisms mentioned above in the quantum Hall effect (QHE) regime. Even though EMPs have been studied in the limit of low temperatures  $k_B T \ll \hbar v_g / \ell_0$ , where  $v_g$  is the group velocity of the edge states and the magnetic length  $\ell_0 = \sqrt{\hbar / m^* \omega_c}$  with  $\omega_c = |e|B / m^* c$ , in the calculation of the current density  $\mathbf{J}$  was assumed that the components of the electric field  $\mathbf{E}$  of the wave are smooth on the  $\ell_0$  scale. However, this assumption can not be well justified for EMPs at very low temperatures. Here, we extend the approach of Refs. [21,22] for not-too-low temperatures, where  $\hbar \omega_c \gg k_B T \gg \hbar v_g / \ell_0$ . In this regime the typical scales of in-plane components of  $\mathbf{E}$  are of the order of  $\ell_T = \ell_0^2 k_B T / \hbar v_g$ , which is much larger than  $\ell_0$ .

Our model to treat EMPs consists in considering a 2DES, of width  $W$ , length  $L_x = L$ , and negligible thickness, in the presence of a strong  $B$  parallel to the  $z$  axis, such that only the  $n = 0$  Landau level (LL) is occupied. The 2DES is confined along the  $y$  axis by a parabolic potential at the edges given by  $V'_y = 0$ , for  $y_l < y < y_r$ ,  $V'_y = m^* \Omega^2 (y - y_r)^2 / 2$  for  $y > y_r > 0$ , and  $V'_y = m^* \Omega^2 (y - y_l)^2 / 2$  for  $y < y_l < 0$ . We assume that the confinement is smooth on the scale of  $\ell_0$  such that  $\Omega \ll \omega_c$  and  $|k_x|W \gg 1$  such that it is reasonable to consider the EMP along the right edge of the channel, in the form  $A(\omega, k_x, y) \exp[-i(\omega t - k_x x)]$ , totally independent of the left edge. We consider the QHE regime, at filling factors  $\nu = 1$  or  $\nu = 2$  in samples with areal dimensions sufficiently large, as it is typical in EMP experiments. So, the inter-edge electron transitions and the inter-edge Coulomb interaction can be neglected. At  $\nu = 1$ , we assume that the spin-splitting, caused by many-body effects, is strong enough to neglect the contribution from the upper spin-split LL. At  $\nu = 2$ , we neglect spin-splitting.

There are at least two essential aspects to take into account in order to determine the dispersion relation as well the spatial structures of the EMPs, One is the role of dissipation even in the QHE regime. Recently it was shown, for sufficiently smooth confinement, that the dissipation comes from the intralevel-intraedge electronic transitions due to scattering by piezoelectric phonons and occurs mainly near the edges of the channel [24]. In the linear response regime, this is the main dissipation mechanism if  $v_g > s$ , the speed of sound, *i.e.*, for channels of width  $W \lesssim 100 \mu\text{m}$

and  $T \lesssim 1$  K. The dissipation in the bulk is exponentially suppressed for  $\hbar\omega_c/k_B T \gg 1$ . So, the properties of the EMPs must be strongly modified when the dissipation is localized near the edges in comparison with previous works in which the dissipation occurs homogeneously over the channel width [13].

The second point is the profile of the unperturbed electron density  $n_0(y)$  across the edge. It was shown that the introduction of a smooth  $n_0(y)$ , considered in Ref. [16], leads to the appearance of new acoustic modes in addition to those found in Ref. [13] in which the electron density drops abruptly at the edge. In Fig. 1, we compare our calculated unperturbed density profile  $n_0(y)$  with the Volkov-Mikhailov [13] and Aleiner-Glazman [16] models. Notice that  $n_0(y)$  is presented on the scale of  $\ell_T \gg \ell_0$  near the edge instead of  $\ell_0$ , as in Fig. 1 of Ref. [22]. Our calculated exact density profile  $n_0(y)/n_0$  (solid curve), where  $n_0$  is the bulk value, is shown together with that of Refs. [13] (short-dashed curve) and [16] (dotted curve). The dash-dotted curve represents our approximate density profile given by  $n_0(y)/n_0 = [1 - \tanh(Y/2)]/2$ , where  $Y = (y - y_{r0})/\ell_T$ . As we can see, our analytical profile is very close to the exact one in the actual region if the condition  $k_e \gg k_B T/\hbar v_g \gg \ell_0^{-1}$  is fulfilled, where the characteristic edge wave number  $k_e = (\omega_c/\hbar\Omega)\sqrt{2m^*}\Delta_F$ , with  $\Delta_F$  being the Fermi energy measured from the bottom of the  $n = 0$  LL, or  $\Delta_F = \overline{E_{F0} - \hbar\omega_c}/2$ . The density profile in the Aleiner-Glazman model is obtained taking  $n_0(y)/n_0 = (2/\pi) \arctan \sqrt{(y_{re} - y)/a}$  and  $a/\ell_0 = 20$  which corresponds approximately to  $a = 2000$  Å. As it can be seen, our density profiles are very different from the other ones. For the calculation of the solid curve, the chosen parameters, related to GaAs-based heterostructures, are  $B = 5.9$  T,  $m^* = 0.067m_0$ ,  $\omega_c/\Omega = 30$ ,  $T = 18$  K,  $\ell_T/\ell_0 = 5$ , and taking  $\Delta_F = \hbar\omega_c/2$  such that  $v_g = \Omega\ell_0 \approx 5 \times 10^5$  cm/sec.

We will show that the combination of our density profile and the fact that dissipation is localized near the edge leads to strong modifications of the EMP behavior. These changes as well as the new EMPs resulting from the present microscopic approach in the regime of not-too-low temperatures are the subject of this work.

The organization of the paper is as follows. In Sec. II, for completeness, we present the expressions for the inhomogeneous current densities and conductivities for not-too-low temperatures and in the quasi-static regime following the treatment given in Ref. [25]. We also obtain the general equation for the EMPs with dissipation at the edges. In contrast with EMPs at very low  $T$ , we neglect the nonlocal contributions to the current density [21,22] since their spatial structure is smooth in the scale of  $\ell_0$ . Further, in Sec. III, we elaborate on the integral equations for symmetric and antisymmetric EMPs and devise a method to solve them. In Sec. IV we derive the dispersion relations and charge-density amplitudes of the symmetric and antisymmetric EMPs and describe in detail the new edge waves. Finally, in Sec. V, we compare our theory with experiment and make concluding remarks.

## II. INTEGRAL EQUATION FOR EMPs WITH DISSIPATION AT THE EDGES

In the low-frequency limit ( $\omega \ll \omega_c$ ) for the EMP, the current density can be calculated in the quasi-static approximation and using the fact that wavelength  $\lambda \gg \ell_0 \lesssim 10^{-6}$  cm and the characteristic scale along  $y$  is typically of the order of  $\ell_T \gg \ell_0$  for not-too-low  $T$  (this condition can be broken only for very high multi-pole modes). Hence the results of Ref. [25] for the components of the current density can be also considered here and are given by

$$j_y(y) = \sigma_{yy}(y)E_y(y) + \sigma_{yx}^0(y)E_x(y), \quad (1)$$

$$j_x(y) = \sigma_{xx}(y)E_x(y) - \sigma_{yx}^0(y)E_y(y) + v_g\rho(\omega, k_x, y). \quad (2)$$

We have suppressed the exponential factor  $\exp[-i(\omega t - k_x x)]$  common to all terms in Eqs. (1) and (2) and obviously  $E_\mu(y)$  depends also on  $\omega$  and  $k_x$ . As shown in Refs. [24] and [25],  $\sigma_{yy}(y)$  is strongly localized with exponential decay at the edge, within a distance  $\lesssim \ell_T$  from it, for  $\hbar\omega_c \gg k_B T \gg \hbar v_g/\ell_0$ . The last term on the right-hand side (RHS) of Eq. (2), absent in Ref. [25], represents the contribution of the current density along  $x$ , associated with the advection of a wave distortion  $\rho(\omega, k_x, y)$  of the charge localized near the edge. For  $\nu = 1$  we have

$$\sigma_{yx}^0(y) = \frac{e^2}{2\pi\hbar} \int_{-\infty}^{\infty} dy_{0\alpha} f_{\alpha 0} \Psi_0^2(y - y_{0\alpha}), \quad (3)$$

where  $\alpha \equiv \{0, k_{x\alpha}\}$ ,  $y_{0\alpha} = \ell_0^2 k_{x\alpha}$ ,  $\Psi_n(y)$  is the harmonic-oscillator function, and  $f_{\alpha 0} \equiv f_0(k_{x\alpha}) = 1/[1 + \exp((E_{\alpha 0} - E_{F0})/k_B T)]$  is the Fermi-Dirac function.  $E_{F0}$  is the Fermi level measured from the bottom of the lowest electric subband. Considering only the flat part of the confining potential,  $y_l \leq y_{0\alpha} \leq y_r$ , we have  $E_{\alpha 0} = \hbar\omega_c/2$ . For the right edge region,  $y_{0\alpha} \geq y_r$ , we obtain

$$E_{\alpha 0} \equiv E_0(y_{0\alpha}) = \hbar\omega_c/2 + m^* \Omega^2 (y_{0\alpha} - y_r)^2/2. \quad (4)$$

In our regime of interest,  $\ell_T \gg \ell_0$ , taking into account that the typical  $y$ -scale of  $f_{\alpha 0}$  and  $\Psi_0^2(y - y_{0\alpha})$  are  $\ell_T$  and  $\ell_0$  respectively, we evaluate the integral in the RHS of Eq. (3) to obtain

$$\sigma_{yx}^0(y) \approx \frac{e^2}{2\pi\hbar} \frac{1}{[1 + \exp((E_0(y) - E_{F0})/k_B T)]}. \quad (5)$$

At the edge of the  $n = 0$  LL,  $y = y_{re} = \ell_0^2 k_{re}$ , where  $f_0(k_{re}) = 1/2$ , we have  $\sigma_{yx}^0(y_{re}) = e^2/(4\pi\hbar)$ . So  $\sigma_{yx}^0(y)$  decreases on the scale of  $\ell_T$  near the edge and behaves like the density profile shown by the solid curve in Fig. 1.

We consider only the electron-phonon interaction, since it is the most essential process for the required conditions [24]. Because the dependence of  $E_x(y)$  on the  $\ell_0$  scale is quite smooth, we can assume that  $\sigma_{xx}(y)$  can be approximated by  $\sigma_{yy}(y)$  and following closely the results of Ref. [25], we can write

$$\begin{aligned} \sigma_{yy}(y) = & \frac{\pi e^2 \ell_0^4}{4\hbar L k_B T} \sum_{k_{x\alpha} \mathbf{q}} |C_{\mathbf{q}}|^2 q_x^2 [f_0(k_{x\alpha} - q_x) - f_0(k_{x\alpha})] \delta[E_0(k_{x\alpha}) - E_0(k_{x\alpha} - q_x) - \hbar\omega_{\vec{q}}] \\ & \times e^{-(q_x^2 + q_y^2)\ell_0^2/2} \sinh^{-2}\left(\frac{\hbar\omega_{\vec{q}}}{2k_B T}\right) [\Psi_0^2(y - y_0(k_{x\alpha} - q_x)) + \Psi_0^2(y - y_0(k_{x\alpha}))]. \end{aligned} \quad (6)$$

For temperatures in the QHE regime, the relevant contributions arise only from acoustical (DA) or piezoelectrical (PA) phonons with dispersion  $\omega_{\mathbf{q}} = sq$ , where  $q = \sqrt{q_x^2 + q_y^2 + q_z^2}$ . Then the interaction strength  $|C_{\mathbf{q}}|^2 = (c'/L_x L_y L_z)q^{\pm 1}$ , where  $+1$  is for DA and  $-1$  for PA-phonons respectively, and  $c'$  is the electron-phonon coupling constant.

Using the Eqs. (1), (2), (5), (6), the Poisson equation and the linearized continuity equation, we obtain the integral equation for  $\rho(\omega, k_x, y)$

$$\begin{aligned} -i(\omega - k_x v_g)\rho(\omega, k_x, y) + \frac{2}{\epsilon} \{k_x^2 \sigma_{xx}(y) - ik_x \frac{d}{dy}[\sigma_{yx}^0(y)] \\ - \sigma_{yy}(y) \frac{d^2}{dy^2} - \frac{d}{dy}[\sigma_{yy}(y)] \frac{d}{dy}\} \int_{-\infty}^{\infty} dy' K_0(|k_x||y - y'|) \rho(\omega, k_x, y') = 0, \end{aligned} \quad (7)$$

where  $K_0(x)$  is the modified Bessel function. We can see from Eqs. (5) and (6) that  $\sigma_{yy}(y)$  and  $d\sigma_{yx}^0(y)/dy$ , as well as  $\sigma_{xx}(y)$ , are exponentially localized within a distance of order of  $\ell_T$  from the right edge at  $y_{re} = y_r + \Delta y_r$  where  $\Delta y_r = \ell_0^2 k_e$  for  $\hbar v_g \ll \ell_0 k_B T$  and  $W = 2y_{re}$ . For  $k_{x\alpha} \equiv k_{re} = y_r/\ell_0^2 + k_e$ ,  $f_0(k_{re}) = 1/2$ , we have

$$v_g = \frac{1}{\hbar} \frac{\partial E_0(k_{re})}{\partial k_{x\alpha}} = \frac{\hbar\Omega^2 k_e}{m^* \omega_c^2} = \sqrt{\frac{2\Delta_F}{m^*}} \frac{\Omega}{\omega_c}. \quad (8)$$

or alternatively  $v_g = cE_e/B$ , where  $E_e = \Omega\sqrt{2m^*\Delta_F}/|e|$  is the electric field describing the influence of the confining potential. For a dissipationless classical 2DES we have, for finite  $\omega$ ,  $\sigma_{yy}(y) = \sigma_{xx}(y) = ie^2 n_0(y)\omega/m^*(\omega^2 - \omega_c^2)$  and  $\sigma_{yx}^0(y) = -e^2 n_0(y)\omega_c/m^*(\omega^2 - \omega_c^2)$ , where  $n_0(y)$  is the electron density. In this case, Eq. (7) is the same as Eq. (4) of Ref. [16].

Equation (7) is valid for a 2DES in the absence of metallic gates. Experimentally, a metallic gate is sometimes placed on the top of the sample at a distance  $d$  from the 2DES [9]. For the gated sample, the kernel  $K_0$  in Eq. (7) is replaced by  $R_g = K_0(|k_x||y - y'|) - K_0(|k_x|\sqrt{(y - y')^2 + 4d^2})$  and if we have air in the top of the 2DES, then  $K_0$  is replaced by  $R_a = K_0(|k_x||y - y'|) + [(\epsilon - 1)/(\epsilon + 1)]K_0(|k_x|\sqrt{(y - y')^2 + 4d^2})$  [21]. For definiteness, we take the background dielectric constant  $\epsilon$  to be spatially homogeneous.

### III. TEMPERATURE EFFECTS ON DISPERSION EQUATIONS FOR EMPS

At temperatures such that the inequality  $k_e \gg k_B T/\hbar v_g \gg \ell_0^{-1}$  is satisfied, we obtain, from Eq. (5), that  $d\sigma_{yx}^0(y)/dy = (e^2/2\pi\hbar)R_0(y)$ , where the function  $R_0(y) = -d[1 + \exp((E_0(y) - E_{F0})/k_B T)]^{-1}/dy \approx (4\ell_T)^{-1} \cosh^{-2}(\bar{y}/2\ell_T)$ , with  $\bar{y} = y - y_{re}$ , is exponentially localized around  $y_{re}$  within a distance of the order of  $\ell_T$ . In addition, from Eq. (6), it follows that the dissipative components of the conductivity tensor  $\sigma_{\mu\mu}(y)$  are proportional to  $R_0(y) \equiv R_0(\bar{y})$ , where  $\mu$  stands for  $x$  or  $y$ , and are also strongly concentrated nearby  $y_{re}$ . Notice also that the condition  $k_e \ell_0 \gg 1$  also holds, due to the fact that  $\omega_c/\Omega \gg 1$  if  $\Delta_F \approx \hbar\omega_c/2$ . Taking into account that only the interaction with PA-phonons is relevant for  $v_g \geq s$ , from Eq. (6) for  $\nu = 1$  we obtain

$$\tilde{\sigma}_{\mu\mu} = \sigma_{\mu\mu}(y)/R_0(\bar{y}) = \frac{e^2 \ell_0^2 c' k_B T}{4\pi^2 \hbar^4 v_g^3}, \quad (9)$$

where, for GaAs-based heterostructures,  $c' = \hbar(eh_{14})^2/2\rho_V s$ , with  $h_{14} = 1.2 \times 10^7$  V/cm,  $\rho_V = 5.31$  gm/cm<sup>3</sup>, and  $s = 2.5 \times 10^5$  cm/sec. Hereafter in numerical estimates and figures we are using these parameters.

One can see also, from Eq. (7), that  $\rho(\omega, k_x, y) \equiv \rho(\omega, k_x, \bar{y})$  is also concentrated near the edge of the  $n = 0$  LL within a region of the order of  $\ell_T$ . Hereafter we use the dimensionless variable  $Y = \bar{y}/\ell_T$ . Furthermore, Eq. (7) is invariant with respect to change  $\bar{y} \rightarrow -\bar{y}$  for even EMP modes, i.e. for which  $\rho(\omega, k_x, \bar{y}) = \rho(\omega, k_x, -\bar{y})$ , or for odd EMP modes,  $\rho(\omega, k_x, \bar{y}) = -\rho(\omega, k_x, -\bar{y})$ . It means that spatially symmetric (even) and spatially antisymmetric (odd) EMP modes of Eq. (7), with respect to  $n = 0$  LL edge  $y_{re}$ , are totally independent from each other. As we will see, it is reasonable to look for a solution of Eq. (7) in a expansion series in terms of Laguerre polynomials  $L_n(Y)$  in the orthogonality interval  $0 \leq Y \leq \infty$ . We define  $\tilde{R}_0(Y) \equiv \exp(Y) * R_0(Y) = [\exp(Y)/4\ell_T] \cosh^{-2}(Y/2)$  and we can see that  $\tilde{R}_0(Y)$  corresponds to the unperturbed electron density profile, which we approximate it by  $n_0(Y)/n_0 = [1 - \tanh(Y/2)]/2$ , which as we have seen practically coincide with the exact one, given by  $2\pi\hbar\sigma_{yx}^0(y)/e^2$ , where  $\sigma_{yx}^0(y)$  is given by Eq. (5), if the conditions  $k_e \gg k_B T/\hbar v_g \gg \ell_0^{-1}$  are fulfilled. Then, from Eq. (7), we obtain the integral equation for symmetric EMPs for  $Y \geq 0$  as

$$\begin{aligned} (\omega - k_x v_g) \rho_s(\omega, k_x, \bar{y}) - \frac{2}{\epsilon} \{ (k_x \sigma_{yx}^0 - i k_x^2 \tilde{\sigma}_{xx}) R_0(\bar{y}) + i \tilde{\sigma}_{yy} \frac{d}{d\bar{y}} [R_0(\bar{y}) \frac{d}{d\bar{y}}] \} \\ * \int_0^\infty d\bar{y}' [K_0(|k_x||\bar{y} - \bar{y}'|) + K_0(|k_x||\bar{y} + \bar{y}'|)] \rho_s(\omega, k_x, \bar{y}') = 0, \end{aligned} \quad (10)$$

In the long-wavelength limit,  $k_x \ell_T \ll 1$ , and for not too strong dissipation at least one EMP mode must have a spatial behavior proportional to  $R_0(Y)$  and for large  $Y$ ,  $\rho_s(\omega, k_x, \bar{y})$  also looks like  $R_0(Y)$ . Then, we write the solution of Eq.(10) for the symmetric EMPs for  $\bar{y} \geq 0$  as

$$\rho_s(\omega, k_x, \bar{y}) = \tilde{R}_0(Y) e^{-Y} \sum_{n=0}^{\infty} \rho_s^{(n)}(\omega, k_x) L_n(Y). \quad (11)$$

For  $\bar{y} \leq 0$ , the expression for  $\rho_s(\omega, k_x, \bar{y})$  follows trivially from Eq. (11), just using  $|Y|$  in the RHS of Eq. (11). Notice that this expansion is valid only when the lowest LL is occupied. We point out that  $\tilde{R}_0(Y)$  is a rather weak dependence on  $Y$ , especially for  $Y \geq 1$ , and tends to  $1/4\ell_T$  as  $Y \rightarrow \infty$ .

In order to obtain the dispersion equation for the symmetric modes, we now multiply Eq. (10) by  $L_m(Y) \tilde{R}_0^{-1}(Y)$  and integrate over  $Y = \bar{y}/\ell_T$  from 0 to  $\infty$ . Then, taking into account the Eq. (11), we obtain

$$(\omega - k_x v_g) \rho_s^{(m)}(\omega, k_x) - \sum_{n=0}^{\infty} [S r_{mn}^s(k_x) + S' g_{mn}^s(k_x)] \rho_s^{(n)}(\omega, k_x) = 0, \quad (12)$$

where, by assuming  $\nu = 1$ ,  $S = (2/\epsilon)(k_x \sigma_{yx}^0 - i k_x^2 \tilde{\sigma}_{xx})$ , with  $\sigma_{yx}^0 = e^2/2\pi\hbar$ ,  $S' = -2i\tilde{\sigma}_{yy}/\epsilon\ell_T^2$ ,

$$r_{mn}^s(k_x) = \ell_T \int_0^\infty dx e^{-x} L_m(x) \int_0^\infty dx' [K_0(|k_x \ell_T||x - x'|) + K_0(|k_x \ell_T||x + x'|)] \tilde{R}_0(x') e^{-x'} L_n(x'), \quad (13)$$

and

$$\begin{aligned} g_{mn}^s(k_x) = |k_x| \ell_T^2 \int_0^\infty dx e^{-x} \{ e^{-x/2} L_m(x) / \cosh(x/2) - \frac{m}{x} [L_m(x) - L_{m-1}(x)] \} \\ \int_0^\infty dx' [\text{sign}\{x - x'\} K_1(|k_x| \ell_T |x - x'|) + K_1(|k_x| \ell_T (x + x'))] \tilde{R}_0(x') e^{-x'} L_n(x'). \end{aligned} \quad (14)$$

Here  $\text{sign}\{x\} = 1$  for  $x > 0$  and  $\text{sign}\{x\} = -1$  for  $x < 0$ , and  $K_1(x)$  is the modified Bessel function. Notice that  $r_{mn}^s \neq r_{nm}^s$  and  $g_{mn}^s \neq g_{nm}^s$ .

Now we consider the antisymmetric EMPs. From Eq. (7), we obtain the following integral equation for  $\rho_a(\omega, k_x, \bar{y})$

$$\begin{aligned} (\omega - k_x v_g) \rho_a(\omega, k_x, \bar{y}) - \frac{2}{\epsilon} \{ (k_x \sigma_{yx}^0 - i k_x^2 \tilde{\sigma}_{xx}) R_0(\bar{y}) + i \tilde{\sigma}_{yy} \frac{d}{d\bar{y}} [R_0(\bar{y}) \frac{d}{d\bar{y}}] \} \\ \int_0^\infty d\bar{y}' [K_0(|k_x||\bar{y} - \bar{y}'|) - K_0(|k_x||\bar{y} + \bar{y}'|)] \rho_a(\omega, k_x, \bar{y}') = 0, \end{aligned} \quad (15)$$

for  $\bar{y} \geq 0$ . As before, we write the exact solution of Eq. (15) for the antisymmetric EMPs as

$$\rho_a(\omega, k_x, \bar{y}) = \tilde{R}_0(Y) e^{-Y} \sum_{n=0}^{\infty} \rho_a^{(n)}(\omega, k_x) L_n(Y), \quad (16)$$

which must satisfy physically obvious boundary condition  $\rho_a(\omega, k_x, 0) = 0$ , which insures continuity of the  $\rho_a(\omega, k_x, \bar{y})$  in the vicinity of  $\bar{y} = 0$ ; i.e., both for  $\bar{y} \rightarrow +0$  and  $\bar{y} \rightarrow -0$ . The odd parity of  $\rho_a(\omega, k_x, \bar{y})$  imposes the following condition on  $\rho_a^{(n)}(\omega, k_x)$

$$\sum_{n=0}^{\infty} \rho_a^{(n)}(\omega, k_x) = 0. \quad (17)$$

For  $\bar{y} < 0$ ,  $\rho_a(\omega, k_x, \bar{y})$  can be obtained from Eq. (16) using the property  $\rho_a(\omega, k_x, x) = -\rho_a(\omega, k_x, -x)$ .

To obtain the dispersion equations for antisymmetric modes, we multiply Eq. (15) by  $L_m(Y) \tilde{R}_0^{-1}(Y)$  and integrate over  $Y = \bar{y}/\ell_T$  from 0 to  $\infty$ . Then, taking into account the Eq. (16), we obtain

$$(\omega - k_x v_g) \rho_a^{(m)}(\omega, k_x) - \sum_{n=0}^{\infty} [S r_{mn}^a(k_x) + S' g_{mn}^a(k_x)] \rho_a^{(n)}(\omega, k_x) = 0, \quad (18)$$

where

$$r_{mn}^a(k_x) = \ell_T \int_0^{\infty} dx e^{-x} L_m(x) \int_0^{\infty} dx' [K_0(|k_x| \ell_T |x - x'|) - K_0(|k_x| \ell_T |x + x'|)] \tilde{R}_0(x') e^{-x'} L_n(x'), \quad (19)$$

and

$$\begin{aligned} g_{mn}^a(k_x) = & |k_x| \ell_T^2 \int_0^{\infty} dx e^{-x} \{ e^{-x/2} L_m(x) / \cosh(x/2) - \frac{m}{x} [L_m(x) - L_{m-1}(x)] \} \\ & \int_0^{\infty} dx' [\text{sign}\{x - x'\} K_1(|k_x| \ell_T |x - x'|) - K_1(|k_x| \ell_T (x + x'))] \tilde{R}_0(x') e^{-x'} L_n(x') + \\ & 2|k_x| \ell_T^2 \int_0^{\infty} dx K_1(|k_x| \ell_T x) \tilde{R}_0(x) e^{-x} L_n(x). \end{aligned} \quad (20)$$

In addition to above equations we must consider the condition given by Eq. (17) that is essential to eliminate the logarithmic divergence in the last integral in the RHS of Eq. (20) after the pertinent summation over  $n$  in Eq. (18). We point out that  $r_{mn}^a \neq r_{nm}^a$ ,  $g_{mn}^a \neq g_{nm}^a$  and hereafter we write  $r_{mn}^{s,a}(k_x) \equiv r_{mn}^{s,a}$  and  $g_{mn}^{s,a}(k_x) \equiv g_{mn}^{s,a}$  to simplify the notation.

In our solution of Eqs. (12)-(20), we are taking the long-wavelength limit  $|k_x| \ell_T \ll 1$ , so we can use the approximations  $K_0(|k_x| \ell_T x) \approx \ln(2/|k_x| \ell_T) - \gamma - \ln(x)$  and  $K_1(|k_x| \ell_T x) \approx (|k_x| \ell_T x)^{-1}$ , where  $\gamma$  is the Euler constant.

## IV. SYMMETRIC AND ANTISYMMETRIC EMPs AT NOT-TOO-LOW TEMPERATURES

### A. Symmetric modes

Considering only the term  $n = 0$  in the RHS of Eq. (11) and for  $m = 0$  in Eq. (12), we obtain

$$[(\omega - k_x v_g) - S r_{00}^s - S' g_{00}^s] \rho_s^{(0)}(\omega, k_x) = 0, \quad (21)$$

where

$$r_{00}^s = \ln\left(\frac{2}{|k_x| \ell_T}\right) - \gamma - \frac{1}{4} \int_0^{\infty} dx e^{-x} \int_0^{\infty} dx' \frac{\ln(|x - x'|) + \ln(x + x')}{\cosh^2(x'/2)}, \quad (22)$$

and a numerical evaluation gives  $g_{00}^s \approx 0.120$ . After performing the integrals in Eq. (22), we have  $r_{00}^s = \ln(1/|k_x| \ell_T) - 0.012 \approx \ln(1/|k_x| \ell_T)$ . Then the dispersion relation (DR) can be written as

$$\begin{aligned}\omega &= k_x v_g + \ln\left(\frac{1}{|k_x| \ell_T}\right) S + 0.12 S' \\ &\approx k_x v_g + \frac{2}{\epsilon} [k_x \sigma_{yx}^0 \ln\left(\frac{1}{|k_x| \ell_T}\right) - 0.12 i \frac{\tilde{\sigma}_{yy}}{\ell_T^2}],\end{aligned}\quad (23)$$

where a quadratic contribution  $\propto k_x^2 \tilde{\sigma}_{xx} \ln(1/|k_x| \ell_T)$  to the damping was neglected because we are considering the long-wavelength limit. Corresponding to the DR of Eq. (23),  $\rho_s(\omega, k_x, \bar{y})$  behaves as  $\cosh^{-2}(Y/2)$ , i.e., without any node. As a consequence, this is the DR of the fundamental EMP at not-too-low temperatures. Furthermore, from Eqs. (23) and (9), it follows that the damping rate of the fundamental EMP in this temperature regime is proportional to  $T^{-1}$  which is essentially different from that at low temperatures [21]. For  $\nu = 2$  the DR of fundamental EMP can be obtained from Eq. (23) by taking  $\sigma_{yx}^0 = e^2/\pi\hbar$  and  $\tilde{\sigma}_{yy} = e^2 \ell_0^2 c' k_B T / (2\pi^2 \hbar^4 v_g^3)$ . Notice that for the same  $E_e$  we have  $\text{Re } \omega(\nu = 2)/\text{Re } \omega(\nu = 1) = 2$ , because  $\ell_T(\nu = 2) = \ell_T(\nu = 1)$  and  $v_g(\nu = 2) = 2v_g(\nu = 1)$  in contrast with the low temperature case [21]. Notice that both expressions for  $\text{Re } \omega$  and  $\text{Im } \omega$ , given by Eq. (23), are essentially different from the results of the Volkov-Mikhailov model [13]. Here the characteristic length of the EMP is  $\ell_T$ , while the characteristic length of a charge for EMP in the cited model is  $\sigma_{yy}^{bu}/k_x \sigma_{yx}^{bu}$ , where  $\sigma_{\mu\gamma}^{bu}$  are the components of the bulk conductivity tensor of the 2DES.

Corrections to the DR of fundamental EMP given by Eq. (23) and the additional *symmetric* branch are obtained by keeping only the terms  $n = 0$  and  $n = 1$  in Eq. (11) which gives

$$\tilde{\rho}_s(\omega, k_x, Y) = \frac{1}{\cosh^2(Y/2)} \left[ 1 + \frac{\rho_s^{(1)}(\omega, k_x)}{\rho_s^{(0)}(\omega, k_x)} L_1(Y) \right], \quad (24)$$

where  $\tilde{\rho}_s(\omega, k_x, Y) = 4\ell_T \rho_s(\omega, k_x, \bar{y})/\rho_s^{(0)}(\omega, k_x)$ . From Eq. (12), for  $m = 0$ , we obtain

$$[(\omega - k_x v_g) - S r_{00}^s - S' g_{00}^s] \rho_s^{(0)}(\omega, k_x) - [S r_{01}^s + S' g_{01}^s] \rho_s^{(1)}(\omega, k_x) = 0, \quad (25)$$

and for  $m = 1$

$$[(\omega - k_x v_g) - S r_{11}^s - S' g_{11}^s] \rho_s^{(1)}(\omega, k_x) - [S r_{10}^s + S' g_{10}^s] \rho_s^{(0)}(\omega, k_x) = 0, \quad (26)$$

The solution of the determinantal equation of the above system yields two branches  $\omega_{\pm}^s(k_x)$  and  $\omega_{\mp}^s(k_x)$ . For  $|k_x| \ell_T \ll 1$ , the numerical evaluation gives  $r_{10}^s = 0.347$ ,  $r_{11}^s = 0.240$ ,  $g_{01}^s = 0.215$ ,  $g_{10}^s = 0.261$ ,  $g_{11}^s = 0.406$ . If we neglect the coupling terms, by formally setting  $r_{01}^s = r_{10}^s = 0$  and  $g_{01}^s = g_{10}^s = 0$ , the Eq. (25) gives the DR of the fundamental EMP, Eq. (23), and, from the Eq. (26), we obtain the DR of the quadrupole EMP, i.e., the EMP with two nodes at  $\bar{y} = \pm \ell_T$ , as

$$\begin{aligned}\omega &= k_x v_g + r_{11}^s S + g_{11}^s S' \\ &\approx k_x v_g + \frac{2}{\epsilon} [0.24 k_x \sigma_{yx}^0 - 0.406 i \frac{\tilde{\sigma}_{yy}}{\ell_T^2}].\end{aligned}\quad (27)$$

The  $\text{Re } \omega$  of the quadrupole EMP at not-too-low temperatures is almost the same as that at low temperatures (cf. Eq. (24) of Ref. [21]), but is essentially different from the frequency of the quadrupole  $j = 2$  branch of the Aleiner-Glazman model [16].

For coupled modes the two branches are given by

$$\begin{aligned}\omega_{\pm}^s &= k_x v_g + \frac{1}{2} [S(r_{00}^s + r_{11}^s) + S'(g_{00}^s + g_{11}^s)] \pm \frac{1}{2} \{ [S(r_{00}^s - r_{11}^s) + \\ &S'(g_{00}^s - g_{11}^s)]^2 + 4(Sr_{01}^s + S'g_{01}^s)(Sr_{10}^s + S'g_{10}^s) \}^{1/2}.\end{aligned}\quad (28)$$

If not stated otherwise, we consider not too strong dissipation, for which  $S \ln(1/|k_x| \ell_T) \gg |S'|$ . In the long wavelength limit, we obtain

$$\omega_{+}^s = k_x v_g + S r_{00}^s + S' g_{00}^s + \frac{(S r_{01}^s + S' g_{01}^s)(S r_{10}^s + S' g_{10}^s)}{S(r_{00}^s - r_{11}^s) + S'(g_{00}^s - g_{11}^s)}, \quad (29)$$

and

$$\omega_{-}^s = k_x v_g + S r_{11}^s + S' g_{11}^s - \frac{(S r_{01}^s + S' g_{01}^s)(S r_{10}^s + S' g_{10}^s)}{S(r_{00}^s - r_{11}^s) + S'(g_{00}^s - g_{11}^s)}. \quad (30)$$

Further, after substituting the coefficients in Eq. (29), we can write

$$\omega_+^s \approx k_x v_g + S r_{00}^s [1 - 1/(7.5 \ln(1/k_x \ell_T))] + S' g_{00}^s [1 - 10/12]. \quad (31)$$

We observe that by taking into account the coupling between the monopole and quadrupole terms  $\text{Re } \omega_+^s$  becomes slightly smaller. However, the damping rate of the fundamental branch is decreased by 6. Finally, we obtain

$$\omega_+^s = k_x v_g + \frac{2}{\epsilon} [k_x \sigma_{yx}^0 \ln(\frac{1}{|k_x| \ell_T}) - i \frac{\tilde{\sigma}_{yy}}{\ell_T^2} (0.02 + k_x^2 \ell_T^2 \ln(\frac{1}{|k_x| \ell_T}))], \quad (32)$$

where in the damping rate the term  $\propto k_x^2$  is returned due to essential suppression of the main contribution to  $\text{Im} \omega_+^s$ . Substituting the DR (31) in Eq. (26) we obtain  $\rho_s^{(1)}(\omega, k_x)/\rho_s^{(0)}(\omega, k_x) \approx (r_{10}^s/r_{00}^s)(1 + 0.75S'/S) \ll 1$ , proving the fast convergence of the expansion for this mode. Now, from the Eq. (24), the charge density for the renormalized fundamental EMP, for  $Y \geq 0$ , can be written as

$$\tilde{\rho}_s(\omega_+^s, k_x, Y) = \frac{1}{\cosh^2(Y/2)} [1 - i \frac{0.26 \tilde{\sigma}_{yy}}{\sigma_{yx}^0 k_x \ell_T^2 \ln(1/|k_x| \ell_T)} L_1(Y)]. \quad (33)$$

We observe that if for some phase  $\phi$  of the wave, its amplitude along  $y$  has a pure monopole character  $\propto \cosh^{-2}(Y/2)$  *i.e.* without any node, after a shift of  $\pm\pi/2$  in  $\phi$ , it acquires a pure quadrupole character  $\propto L_1(|Y|) \cosh^{-2}(Y/2)$  with two nodes at  $Y = \pm 1$ . Because such a behavior can be seen as the rotation of a complex vector function while the wave propagates, we call this fundamental EMP, characterized by the Eqs. (31) and (33), the *edge helicon* (EH) for not-too-low temperatures which has different properties from its counterpart at low temperatures [21].

From Eq. (30) and after substituting the coefficients, the DR of the other branch is given by

$$\omega_-^s \approx k_x v_g + S r_{11}^s [1 + 0.56] + S' g_{11}^s [1 + 1/4]. \quad (34)$$

Now the coupling between quadrupole and monopole terms leads to an increase of 50% in  $\text{Re } \omega_-^s$  and 25% in the damping rate. The ratio between the amplitudes is  $\rho_s^{(1)}(\omega, k_x)/\rho_s^{(0)}(\omega, k_x) \approx 1/[2 \ln(2) - 1] \approx 2.6$  which gives a rather small value for  $\rho_s^{(0)}/\rho_s^{(1)} \approx 1/2.6$  and the convergence of the expansion for the quadrupole mode. Then for renormalized quadrupole mode  $\tilde{\rho}_s(\omega, k_x, Y)$  is given, from Eq. (24), for  $Y \geq 0$  as

$$\tilde{\rho}_s(\omega_-^s, k_x, Y) = \frac{1}{\cosh^2(Y/2)} \{1 + [2 \ln(2) - 1]^{-1} L_1(Y)\}. \quad (35)$$

Due to the coupling between the quadrupole and monopole modes, the nodes of  $\tilde{\rho}_s(\omega, k_x, Y)$  are shifted, in the case of the renormalized quadrupole mode, to  $Y = \pm 2 \ln(2) \approx \pm 1.39$ . Notice that  $\rho_s(Y)$  for both  $Y > 0$  and  $Y < 0$  is given also by Eqs. (33), (35) after the replacement of  $Y$  by  $|Y|$ .

In Fig. 2 the charge density profiles  $\rho(Y)$  of EMPs are depicted for  $\nu = 2$  and  $B = 5.9$  T. The parameters are the same as in Fig. 1 and, when necessary, we took  $k_x \ell_T = 0.1$  and  $\epsilon = 12.5$ . The curves labeled 1 and 2 represent  $\rho(Y) \equiv \rho_s(Y, k_x) = \text{Re} [\tilde{\rho}_s(\omega_+^s, k_x, |Y|) \times \exp(i\phi)]$  for the EH, given by Eq. (33), if the wave phase  $\phi = 2\pi N$  and  $\phi = \pi/2 + 2\pi N$ , where  $N$  is integer, respectively. The curve 3 represents  $\rho(Y) = \tilde{\rho}_s(\omega_-^s, k_x, |Y|)$  for the renormalized quadrupole mode, given by Eq. (35).

## B. Antisymmetric modes

Similar analysis can be done for studying the antisymmetric modes. The DR of the dipole mode at not-too-low temperatures, after taking into account only the terms  $n = 0$  and  $n = 1$  in the RHS of Eq. (16), is given by

$$\begin{aligned} \omega &= k_x v_g + (r_{00}^a - r_{01}^a) S + (g_{00}^a - g_{01}^a) S' \\ &\approx k_x v_g + \frac{2}{\epsilon} [0.65 k_x \sigma_{yx}^0 - 0.5 i \frac{\tilde{\sigma}_{yy}}{\ell_T^2}], \end{aligned} \quad (36)$$

since  $r_{00}^a \approx 0.509$ ,  $r_{01}^a \approx -0.141$  and  $g_{00}^a - g_{01}^a - 1 \approx -0.502$ . The charge amplitude  $\rho_a(\omega, k_x, \bar{y})$  of this dipole mode behaves as  $\tilde{\rho}_a(Y) = 4\ell_T \rho_a(\omega, k_x, \bar{y})/\rho_s^{(1)}(\omega, k_x) = -Y \cosh^{-2}(Y/2)$ , *i.e.*, with one node at  $Y = 0$ . Its density profile

$\rho(Y) \equiv \tilde{\rho}_a(Y)$  corresponds to curve 4 in Fig. 2. The frequency of the dipole EMP,  $\text{Re}(\omega - k_x v_g)/S = 0.65$ , is 30% larger than for the similar mode at low temperatures.

Corrections to the DR of the dipole EMP, given by Eq. (36), and the additional *antisymmetric* branch can also be obtained, by keeping only the terms  $n = 0, 1$  and  $n = 2$  in the RHS of Eq. (16), in a straightforward way. Then we obtain two branches  $\omega_+^a(k_x)$  and  $\omega_-^a(k_x)$ . If we neglect the coupling between different terms of the expansion we obtain, for  $|k_x|\ell_T \ll 1$ , the following expression for the DR of the octupole mode

$$\omega \approx k_x v_g + \frac{2}{\epsilon} [0.14 k_x \sigma_{yx}^0 - 0.205 i \frac{\tilde{\sigma}_{yy}}{\ell_T^2}]. \quad (37)$$

Neglecting dissipation and the  $k_x v_g$  term, the octupole EMP at not-too-low temperatures exhibits a phase velocity around 85% of the phase velocity of the octupole EMP at low temperatures (cf. Eq. (44) of Ref. [21]). Again the frequency of this mode is distinct from the frequency of the octupole  $j = 3$  branch of Ref. [16]. The charge density profile  $\tilde{\rho}_a(Y) = Y(1 - |Y|/2) \cosh^{-2}(Y/2)$ , *i.e.*, with three nodes at  $Y = 0$  and  $Y = \pm 2$  is represented by curve 5 in Fig. 2.

If we consider the coupling between the expansion terms, we obtain the dipole and octupole renormalized modes. Our numerical results have shown that the renormalization effects are quite weak in the regime of not-too-low temperatures which means that, in our theory for high temperature EMPs, the convergence of the expansion, given by Eq. (16), for the dipole and octupole modes is faster than that expansion over Hermitian polynomials used in Ref. [21] in the regime of very low temperatures.

In Fig. 3 we plot the dimensionless electric potential  $\Phi \propto \int_{-\infty}^{\infty} dY' K_0(|k_x|\ell_T|Y - Y'|) \rho(Y')$  for EMPs with the charge density profiles  $\rho(Y)$  denoted by curves 1 to 5 in Fig. 2.

## V. DISCUSSION AND CONCLUDING REMARKS

In this work we have introduced an analytical unperturbed electron density profile  $n_0(Y)/n_0 = [1 - \tanh(Y/2)]/2$  which is in very good agreement with the exact results, as shown in Fig. 1, when the conditions,  $\hbar\omega_c/k_B T \gg 1$ ,  $k_e \gg k_B T/\hbar v_g \gg \ell_0^{-1}$  are fulfilled.

We have shown that temperature effects manifest themselves in the dispersion and spatial structure of the EMP modes by changing the characteristic length to  $\ell_T \gg \ell_0$ . The edge density profiles for dipole, quadrupole, and octupole EMPs in this regime behave spatially independent of the wave phase  $\phi$ . However the behavior of the density profile of the edge helicon is qualitatively modified by varying  $\phi$  as shown in curves 1 and 2 of Fig. 2. Concerning the dissipation of the modes, we introduce the dimensionless parameter  $\eta_T$  as  $\eta_T = \xi/(k_x \ell_T)$ , where  $\xi = \tilde{\sigma}_{yy}/(\ell_T \sigma_{yx}^0) = [e^2 h_{14}^2 / 4\pi \hbar s^3 \rho_V](s^2/v_g^2)$ . Then, we have observed that the regime of *weak dissipation* occurs at  $\eta_T \ll 1$  since  $\text{Re} \omega \gg \text{Im} \omega$  for all modes. The opposite regime of *strong dissipation* corresponds to  $\ln(1/k_x \ell_T) \gg \eta_T \gtrsim 1$  because all modes, except the edge helicon, are strongly damped, *i.e.*,  $\text{Re} \omega \lesssim \text{Im} \omega$ . So the edge helicon is the only weakly damped mode in the region of strong dissipation. We also observe from the comparison between the curves in Fig. 3 and the corresponding ones in Fig. 2 that the wave potential  $\Phi(Y) \propto E_x(\omega, k_x, y)$  is smooth on the scale of the magnetic length both for symmetric and antisymmetric modes even when the charge density profile  $\rho(Y)$  of the EMP shows a cusp in the vicinity of  $Y = 0$ . This smoothness of the EMPs electric potential justifies well the assumptions of our present study.

Finally, we make some estimates that should be useful in experimental studies. For the GaAs-based samples with the parameters used in Fig. 1 and  $k_x \ell_T = 0.1$  ( $k_x \approx 2 \times 10^4 \text{ cm}^{-1}$ ), we obtain  $\xi = 0.353 s^2/v_g^2 \approx 8.8 \times 10^{-2}$  and hence  $\eta_T \approx 0.88$ , which corresponds to the case of *strong dissipation*. We propose here a sample arrangement very similar to that of Ashoori *et al.* [7]. Our circular mesa has a diameter  $D = 15 \mu\text{m}$  (in Ref. [7]  $D = 540 \mu\text{m}$ ) and height  $\sim 1 \mu\text{m}$  in the middle of a wide GaAs/AlGaAs chip with large thickness such that  $2d_s \gg 1/k_x = 0.5 \mu\text{m}$  and we assume as in Ref. [7] the value  $d_s = 500 \mu\text{m}$ . The condition  $2|k_x|d_s \gg 1$  is well satisfied even for  $k_{x0} = 2/D = 1.3 \times 10^3 \text{ cm}^{-1}$ , as the assumed  $k_x \gg k_{x0}$ . As a consequence, the conditions  $2k_x d_s \gg 1$  and  $k_x W \gg 1$  are satisfied as well. Analogous to Ref. [7], we assume that a square “pulsar” gate with width  $L_p \approx 0.8 \mu\text{m}$  ( $L_p = 10 \mu\text{m}$  in Ref. [7]) is much smaller than  $\pi D$ . Furthermore, the initial charge distribution (when a pulse of external voltage is applied to the “pulsar” gate) has a rectangular form and therefore the essential contributions come from the  $k_{xn} = \pm n k_{x0}$ ,  $n = 1, 2, \dots$ , modes distributed in the interval  $k_{x0} \leq |k_{xn}| < \pi/L_p$ . So, a typical wave number  $k_{xt} = |k_{xnt}| \approx \pi/2L_p = 2 \times 10^4 \text{ cm}^{-1}$  is of the same order of the magnitude of our estimated  $k_x$ . As all modes, except one, are strongly damped we are left with the edge helicons. Equation (32) gives a decay rate  $\text{Im} \omega_+^s \approx 7.5 \times 10^9 \text{ sec}^{-1}$ . The corresponding group velocity for this mode is  $v_{g+}(k_{xt}) = v_g + (2/\epsilon)\sigma_{yx}^0 [n(1/k_{xt}\ell_T) - 1]$  and gives a period  $T_+ = \pi D/v_{g+}(k_{xt}) \approx 3.1 \times 10^{-10} \text{ sec}$ . So, during the travelling period  $T_+$ , the amplitude of the mode should drop only by a factor  $\sim \exp(-2.3)$ . As it is known,



the amplitude of the travelling pulse in time-resolved experiments [7] can be measured by another square gate with side  $L_p$  above the edge. So, we believe from our reasonable estimates that the edge helicon mode may be detected.

## ACKNOWLEDGMENTS

This work was supported by Brazilian FAPESP Grants No.98/10192-2 and 95/0789-3. In addition, O. G. B. acknowledges partial support by the Ukrainian SFFI Grant No. 2.4/665, and N. S. is grateful do Brazilian CNPq for a research fellowship.

- 
- [1] D. B. Mast, A. J. Dahm, and A. L. Fetter, Phys. Rev. Lett **54**,1706 (1985).
  - [2] D. C. Glatli, E. Y. Andrei, G. Deville, J. Poitrenaud, and F. I. B. Williams, Phys. Rev. Lett.**54**,1710 (1985).
  - [3] O. I. Kirichek, P. K. H. Sommerfeld, Yu. P. Monarkha, P. J. M. Peters, Yu. Z. Kovdrya, P. P. Steijaert, R. W. van der Heijden, and A. T. A. M. de Waele, Phys. Rev. Lett.**74**,1190 (1995).
  - [4] V. I. Tal'yanskii, I. E. Batov, B. K. Medvedev, J. P. Kotthaus, M. Wassermeier, A. Wixforth, J. Weimann, W. Schlapp, and H. Nickel, Pis'ma Zh. Eksp. Teor. Fiz. **50**, 196 (1989) [JETP Lett. **50**, 221 (1989)].
  - [5] M. Wassermeier, J. Oshinowo, J. P. Kotthaus, A. H. MacDonald, C. T. Foxon, and J. J. Harris, Phys. Rev. B **41**, 10287 (1990).
  - [6] I. Grodnensky, D. Heitmann, and K. von Klitzing, Phys. Rev. Lett. **67**,1019 (1991); Surface Science **263**, 467 (1992).
  - [7] R. C. Ashoori, H. L. Stormer, L. N. Pfeiffer, K. W. Baldwin, and K. West, Phys. Rev. B **45**, 3894 (1992).
  - [8] V. I. Tal'yanskii, A. V. Polisski, D. D. Arnone, M. Pepper, C. G. Smith, D. A. Ritchie, J. E. Frost, and G. A. C. Jones, Phys. Rev. B **46**, 12427 (1992).
  - [9] N. B. Zhitenev, R. J. Haug, K. von Klitzing, and K. Eberl, Phys. Rev. Lett. **71**, 2292 (1993); Phys. Rev. B **49**, 7809 (1994).
  - [10] G. Ernst, R. J. Haug, J. Kuhl, K. von Klitzing, and K. Eberl, Phys. Rev. Lett. **77**, 4245 (1996).
  - [11] N. Balaban, Y. Meirav, H. Shtrikman, and V. Umansky, Phys. Rev. B **55**, R13397 (1997); N. Q. Balaban, Y. Meirav, and I. Bar-Joseph, Phys. Rev. Lett. **81**, 1481 (1998).
  - [12] A. L. Fetter, Phys. Rev. B **33**, 3717 (1986).
  - [13] V. A. Volkov and S. A. Mikhailov, Zh. Eksp. Teor. Fiz. **94**, 217 (1988) [Sov. Phys. JETP **67**, 1639 (1988)]; in *Modern Problems in Condensed Matter Sciences*, edited by V. M. Agranovich and A. A. Maradudin (North-Holland, Amsterdam, 1991), Vol. 27.2, Ch. 15, p. 885.
  - [14] X. G. Wen, Phys. Rev. B **43**, 11025 (1991).
  - [15] M. Stone, Ann. Phys. (NY) **207**, 38 (1991); M. Stone, H. W. Wyld, and R. L. Schult, Phys. Rev. B **45**, 14156 (1992).
  - [16] I. L. Aleiner and L. I. Glazman, Phys. Rev. Lett. **72**, 2935 (1994).
  - [17] C. de Chamon and X. G. Wen, Phys. Rev. B **49**, 8227 (1994).
  - [18] J. S. Giovanazzi, L. Pitaevskii, and S. Stringari, Phys. Rev. Lett. **72**, 3230 (1994).
  - [19] J. H. Han and D. J. Thouless, Phys. Rev. B **55**, R1926 (1997).
  - [20] U. Zulicke, R. Bluhm, V. A. Kostelcky, and A. H. MacDonald, Phys. Rev. B **55**, 9800 (1997).
  - [21] O. G. Balev and P. Vasilopoulos, Phys. Rev. B **56**, 13252 (1997).
  - [22] O. G. Balev and P. Vasilopoulos, Phys. Rev. Lett. **81**, 1481 (1998); O. G. Balev, P. Vasilopoulos, and Nelson Studart, J. Phys.: Condens. Matt. **11**, 5143 (1999).
  - [23] O. G. Balev and P. Vasilopoulos, Phys. Rev. B **59**, 2807 (1999).
  - [24] O. G. Balev and P. Vasilopoulos,(a) Phys. Rev. B **47**, 16410 (1993); (b) ibid. **50**, 8706 (1994); (c) ibid. **50**, 8727 (1994).
  - [25] O. G. Balev and P. Vasilopoulos, Phys. Rev. B **54**, 4863 (1996).

## FIGURE CAPTIONS

FIG. 1. Unperturbed electron density  $n_0(y)$ , normalized to the bulk value  $n_0$ , as a function of  $Y = (y - y_{r0})/\ell_T$ , where  $y_{r0}$  is the edge of  $n = 0$  LL. The solid and dash-dotted curves show our exact and approximate profiles, respectively, for a GaAs-based heterostructure and for  $\nu = 2$ ,  $B = 5.9\text{T}$ ,  $\omega_c/\Omega = 30$ ,  $\Delta_F = \hbar\omega_c/2$ ,  $\ell_T/\ell_0 = 5$ , and  $T = 18\text{ K}$ . The dashed curve is the density profile in the model of Ref. [13] and the dotted curve that of Ref. [16] for  $n_0(y)/n_0 = (2/\pi) \arctan[(y_{re} - y)/a]^{1/2}$ ,  $a/\ell_0 = 20$ . For the dashed and the dotted curves  $Y = (y - y_{re})/\ell_T$ , where  $y_{re}$  is the edge in the models of Refs. [13] and [16].

FIG. 2. Dimensionless charge density profile  $\rho(Y)$  of EMPs at not-too-low temperatures: curves 1, 2, and 3 correspond to symmetric modes and curves 4 and 5 to the antisymmetric ones. Curves 1 and 2 represent  $\rho(Y)$  for the edge helicon, using Eq. (33), for different wave phases and curve 3 represents  $\rho(Y)$  for the renormalized quadrupole EMP, Eq. (35). Curves 4 and 5 are  $\rho(Y)$  for dipole and octupole EMPs, respectively. The parameters are the same as in Fig. 1.

FIG. 3. Dimensionless electric potential  $\Phi(Y)$  of EMPs at not-too-low temperatures. Curves 1 to 5 correspond to charge profiles labeled in Fig. 2.

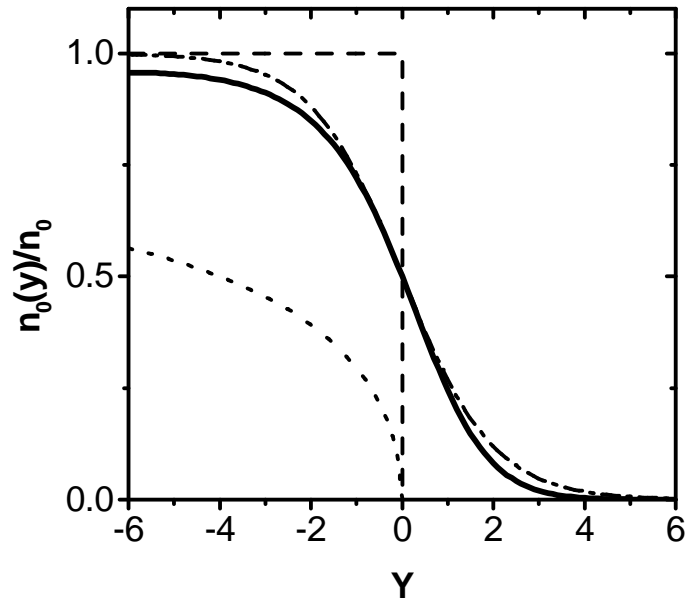


Fig. 1

Balev O. G. *et al.*

"Temperature effects on edge magnetoplasmons in ..."

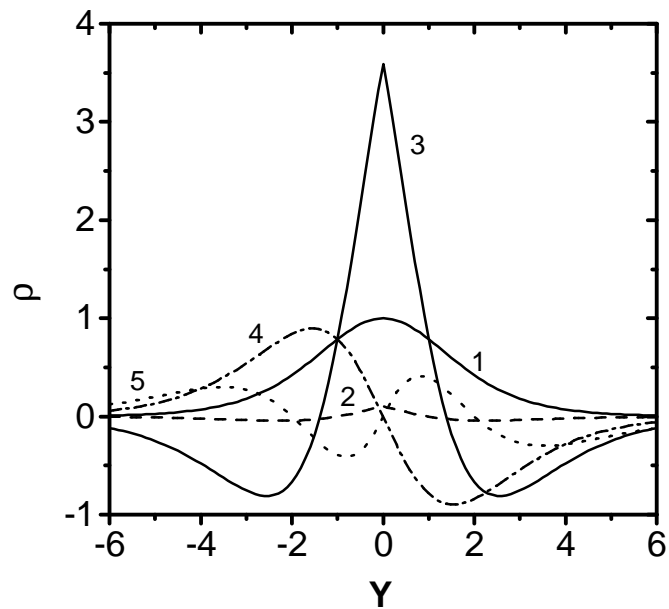


Fig. 2

Balev O. G. *et al.*

"Temperature effects on edge magnetoplasmons in ..."

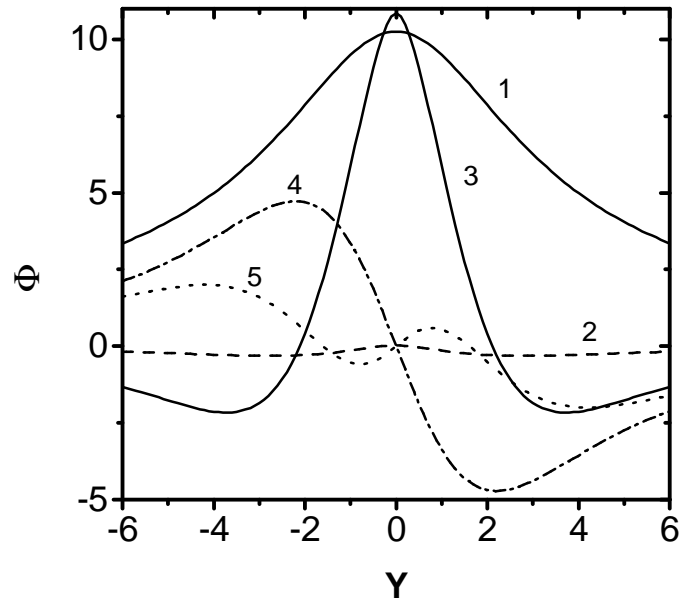


Fig. 3

Balev O. G. *et al.*

"Temperature effects on edge magnetoplasmons in ..."